Journal of Sound and Vibration (2001) **239**(2), 275–295
doi:10.1006/jsvi.2000.3159, available online at http://www.idealibrary.com on IDEAL®

POWER FLOW ANALYSIS OF COMPLEX COUPLED SYSTEMS BY PROGRESSIVE APPROACHES

Y. P. XIONG

Institute of Engineering Mechanics, Shandong University of Technology, Jinan, 250061, People's Republic of China

School of Engineering Sciences, Ship Science, University of Southampton, Southampton SO17 1BJ, U.K.
E-mail: xiongyp@dms.sdut.edu.cn

AND

J. T. XING AND W. G. PRICE

School of Engineering Sciences, Ship Science, University of Southampton, Southampton SO17 1BJ, U.K.
E-mail: j.t.xing@ship.soton.ac.uk

(*Received* 9 *March* 2000, *and in final form* 30 *May* 2000)

A generalized mobility/impedance-power flow mathematical model is developed to analyze the dynamical behaviour of a complex coupled system consisting of any number of substructures with various configurations and multiple interaction interfaces. The coupled system is subject to multiple excitations and selected boundary conditions. Generalized mobility/impedance matrix formulations for three-dimensional rigid and elastic structures of general configuration are first derived allowing the construction of *equivalent mobility* (EMM) and *equivalent impedance* (EIM) matrices to describe the dynamical behaviour of a substructure or a subsystem assembled from several inter-connected substructures within the overall system. Based on these two proposed matrices, two progressive approaches are developed to predict the force vectors and velocity response vectors as well as the power flows into and transmission between substructures in the complex coupled system. The developed mathematical model avoids the generalized inverse process associated with rectangular matrices when dealing with multi-input/multi-output (MIMO) systems in which the dimensions of input and output are different. It is also very flexible and conveniently extended if additional substructures are further connected to the original dynamic system without involving much additional computational effort. The proposed methods are shown to reduce the complexity of the power flow analysis applied to complex dynamic coupled systems and they are applicable to a very large class of dynamical systems in engineering. To illustrate and demonstrate their usage, the dynamics of a flexible raft vibration isolation system is investigated; this comprises two machines, flexible raft, and flexible foundation with connecting isolator attachments.

1. INTRODUCTION

Power flow analysis (PFA) or statistical energy analysis (SEA) has become widely accepted as a valuable technique to predict statistical responses of dynamic systems and vibrational power flows through structures or assembled structures at medium to high frequencies [1–23]. The fundamental concepts of SEA and PFA have been discussed by Lyon [1], Price and Keane [2], Goyder and White [5–7] and Pinnington and White [8, 9], with significant advances reported in recent publications [2–4]. Langley [10] presented a direct-dynamic

0022-460X/01/020275 + 21 $35.00/0

stiffness method to analyze the power flow in beams and frameworks. Clarkson [11] applied the receptance method to investigate the transmission of vibrational energy across structural joints of connected beams and connected plates. Mead *et al.* [12] studied power transmission in a periodically supported infinite beam subject to a single excitation. Cuschieri [13, 14] used a mobility approach to analyze the power flow in periodically connected beams and *L*-plates subject to a single excitation. Farag and Pan [15] extended Cuschieri's work to coupled two-dimensional beam structures with multiple joints under in-plane loading. The mobility functions of vacuous elastic cylindrical shells were numerically studied by Ming *et al.* [16] and applied to estimate both the input power and the power flow in coupled finite cylindrical shell systems. Gardonio *et al.* [17] presented a model of vibration isolation systems by developing a matrix method using mobility or impedance representations of three separate elements: the source of vibration, the receiver and the mounting system and investigated five different active control strategies to reduce the structural power transmission from a source to a receiver via a number of active mounts [18]. Cho and Bernhard [19] developed a governing energy differential equation to describe the far field vibrational energy state and to predict the frequency-averaged energy per unit length and energy flow distributions in built-up structures. The transmission of vibratory power flow from a vibrating rigid body into a thin supported panel through two mounts was investigated by Pan *et al.* [20]. Li *et al.* [21] studied a more complex case concerning the transmission of vibration power flow from a vibrating rigid machine into a rectangular plate with a number of reinforcing beams placed in any directions. Li *et al.* [22] studied power flow for a simple floating beam-like raft isolation system with one machine subject to a single harmonic force excitation using a Green function. Investigations relating to a power flow analysis mainly focus on individual structures, coupled beam- or plate-like structures or periodic systems. From the more generic viewpoint of continuum mechanics, Xing and Price [23] developed a power flow analysis method based on continuum dynamics. The characteristics of energy flow and energy exchange within the continuum were described through the introduction of concepts such as an energy flow line and an energy flow potential, equipotential surface, etc. The generalized power flow equations describing the characteristics of energy flow and energy exchange within the continuum are presented; however, the solution of these equations directly to obtain power flow distributions requires further study.

Many techniques are presented in the literature to predict dynamic characteristics of coupled systems composed of various subsystems, e.g. receptance theory [24] frequency response function (FRF), transfer matrix, the four-pole parameter method, etc. The FRF method [25] is more suitable to a system consisting of only two subsystems. If additional subsystems are further connected to the original system, computational effort to derive solution greatly increases. The four-pole parameter method [26, 27] is a classical technique for deriving dynamic characteristics of an assembled system connected in series or in parallel. Although this method was originally limited to unidirectional single-input/single-output (SISO) linear mechanical systems, recently, however, Ha and Kim [28] and Xiong [29] extended the four-pole parameter method to multiple-input/multiple-output (MIMO) linear systems. However, when assembling substructures in these systems with different inputs and outputs, generalized inverse or pseudo-inverse [30] processes associated with rectangular four-pole parameter matrices are required to examine or to estimate coupling interactions [28,29]. This causes increased complexity in the mathematical model and subsequent solution.

Mobility matrices describing the dynamic characteristics of some typical elements, such as, rod, shaft, beam and plate, etc., are very useful in calculating structural power flows [12–22]. However, they are not readily available when analyzing complex coupled systems,

especially with various and differing configurations. In this paper, to overcome such difficulty, generalized mobility and impedance matrices for three-dimensional rigid and elastic structures are derived. Based on this information, *equivalent mobility* and *equivalent impedance* matrices are introduced to describe the dynamical behaviour of a subsystem assembled from several inter-connected substructures within the overall system. Furthermore, two progressive approaches are developed to predict force vector, velocity response vector and power flows transmitted between substructures in a complex coupled system consisting of n substructures subject to selected boundary conditions and multiple excitations. The proposed methods are very efficient and greatly reduce the complexity of the power flow analysis when examining complex dynamic, coupling systems. For the special case of periodic systems, where the substructures are identical, these methods become even more effective. To demonstrate the application of the proposed generalized approaches, the dynamics of a flexible raft vibration isolation system is investigated.

2. DESCRIPTION OF A DYNAMIC COUPLED SYSTEM MODEL

Figure 1(a) illustrates schematically a generalized complex coupled system with n subsystems S_k $(k = 1, 2, \ldots, n)$, where each substructure represents either a rigid or flexible component of the global system, or several different components in one substructure. The rigid component possesses six degrees of freedom, whereas a flexible structure subject to various boundary conditions admits multiple degrees of freedom. A representative substructure S_k with r_k inputs and r_{k+1} outputs within the global system is shown in Figure 1(b).

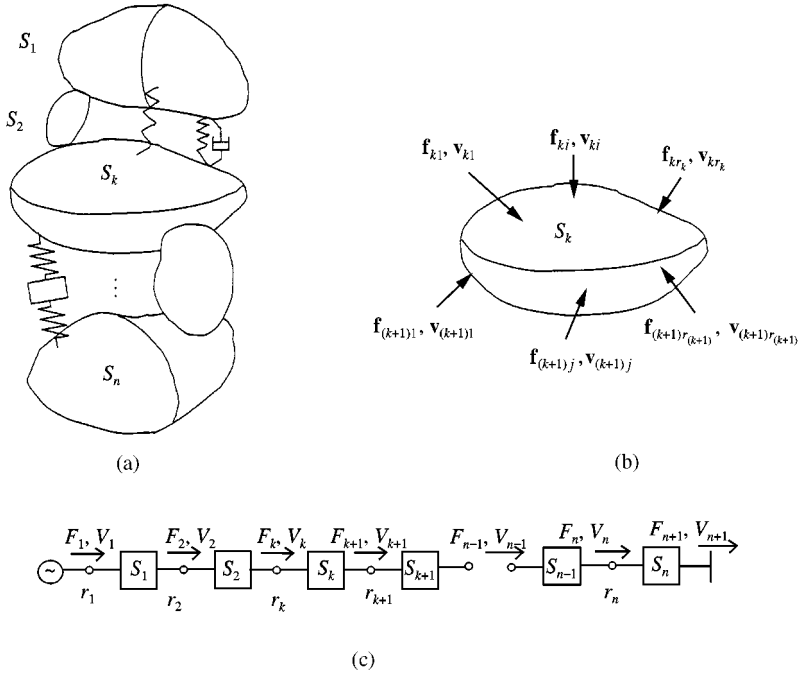

Figure 1. A general multiple input–output dynamic coupling system. (a) Global system; (b) a representative substructure S_k $(k = 1, 2, \ldots, n)$ with r_k inputs and r_{k+1} outputs; (c) a symbolic representation of the coupled systems with n substructures.

The kth substructure S_k is connected to substructures S_{k-1} and S_{k+1}, through generalized interfacial force vectors denoted by $\mathbf{F}_k$ and $\mathbf{F}_{k+1}$ respectively.

As its practical case is that a moment is added to a structure always through a couple of forces with equal magnitude but opposite direction applied at two positions or a distribution force, which can be approximated by several concentrated forces as used in finite element analysis, on a surface of the structure, one can represent each input vibration excitation by the force vector $\mathbf{f}_{kj} = \{f_{xj}, f_{yj}, f_{zj}\}^{\mathrm{T}}$ $(j = 1, 2, \ldots, r_k)$. In general, therefore, all excitation forces can be represented by the generalized force vector $\mathbf{F}_k = \{\mathbf{f}_{k1}, \ldots, \mathbf{f}_{kj}, \ldots, \mathbf{f}_{kr_k}\}^{\mathrm{T}}$. The corresponding velocity response vector is denoted by $\mathbf{V}_k = \{\mathbf{v}_{k1}, \ldots, \mathbf{v}_{kj}, \ldots, \mathbf{v}_{kr_k}\}^{\mathrm{T}}$, where each velocity vector is represented by $\mathbf{v}_{kj} = \{v_{xj}, v_{yj}, v_{zj}\}^{\mathrm{T}}$ $(j = 1, 2, \ldots, r_k)$. Similarly, the generalized output force and velocity vectors are represented by $\mathbf{F}_{k+1}$ and $\mathbf{V}_{k+1}$ respectively. Figure 1(c) shows a symbolic representation of a coupled system with n substructures. General, combined dynamic excitations are accounted for in the mathematical model and they relate to vibrations caused not only by force or motion excitations applied to substructure S_1 but also force or motion excitations of the supporting substructure S_n. For example, for different prescribed boundary conditions, the dynamic coupling problems represented by Figure 1(c) can be categorized into the following four cases:

Case 1: $\mathbf{F}_1 = \hat{\mathbf{F}}_1$, $\mathbf{V}_{n+1} = \hat{\mathbf{V}}_{n+1}$. The system is excited by a prescribed force vector $\mathbf{F}_1 = \{\mathbf{f}_{11}, \ldots, \mathbf{f}_{1j}, \ldots, \mathbf{f}_{1r_1}\}^{\mathrm{T}}$ acting on substructure S_1 and a prescribed velocity vector $\mathbf{V}_{n+1}$ of substructure S_n, or the boundary output velocity responses of S_n to have given values. Substructure S_1 may represent one or a group of vibrating machines on which the force vector $\mathbf{F}_1 = \{\mathbf{f}_{11}, \mathbf{f}_{12}, \ldots, \mathbf{f}_{1j}, \ldots, \mathbf{f}_{1r_1}\}^{\mathrm{T}}$ is a prescribed force vector $\hat{\mathbf{F}}_1$ consisting of r_1 harmonic excitation sources of frequency ω, i.e., $\mathbf{F}_1 = \hat{\mathbf{F}}_1$. Substructure S_n represents a flexible supporting structure either fixed to a rigid foundation with $\mathbf{V}_{n+1} = \mathbf{0}$ or subject to a motion excitation associated with a prescribed velocity vector $\mathbf{V}_{n+1} = \hat{\mathbf{V}}_{n+1}$. For example, a multi-storey building is excited by installed machinery mounted on its top floor such as air conditioning equipment and its auxiliaries, and excited by seismic excitations at its foundation. A floating raft vibration isolation system is another engineering application of this case with $\mathbf{F}_1 = \hat{\mathbf{F}}_1$, $\hat{\mathbf{V}}_{n+1} = \mathbf{0}$.

Case 2: $\mathbf{V}_1 = \hat{\mathbf{V}}_1$, $\mathbf{V}_{n+1} = \hat{\mathbf{V}}_{n+1}$. This case may represent vibrations in the system caused by motion of substructure S_1 and by prescribed boundary velocity vector $\mathbf{V}_{n+1}$ of substructure S_n. It may also imply that either the input velocity responses of S_1 or the output velocity responses of S_n are imposed constraints. Examples of its engineering applications are passive vibration isolation systems and packaging dynamic systems where the excitation is caused by the motion of the foundation structure.

Case 3: $\mathbf{F}_1 = \hat{\mathbf{F}}_1$, $\mathbf{F}_{n+1} = \hat{\mathbf{F}}_{n+1}$. This system is excited by force vectors acting on substructure S_1 and substructure S_n, with no motion constraints assumed on the boundaries. Typical applications of this analysis are found in ships or submarines subject to multiple excitations by engine, auxiliary machinery and sea waves. Similarly, when analyzing aeroplane vibrations, aerodynamic forces and engines are sources of force excitations.

Case 4: $\mathbf{V}_1 = \hat{\mathbf{V}}_1$, $\mathbf{F}_{n+1} = \hat{\mathbf{F}}_{n+1}$. This case is similar to Case 1 with roles and the numbering of the system reversed.

3. GENERALIZED MOBILITY AND IMPEDANCE MATRICES OF SUBSTRUCTURES

For a complex global structure in which all substructures are different, a general mobility or impedance matrix of individual substructures is required to characterize the dynamic

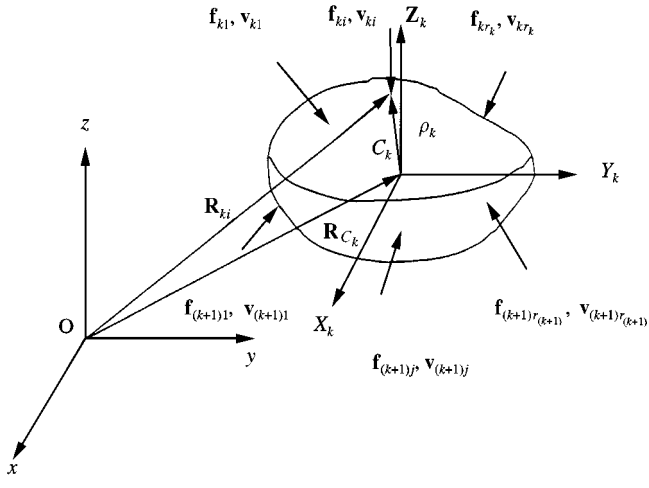

Figure 2. Local and global co-ordinate systems and force and velocity vectors acting on the rigid substructure S_k.

coupling behaviour of the system. In this section, generalized mobility or impedance matrix formulations for three-dimensional rigid and elastic structures are derived allowing description of the dynamical coupling behaviour of a subsystem assembled from several inter-connected substructures within the overall system.

3.1. RIGID-BODY SUBSTRUCTURE

Figure 2 illustrates a general three-dimensional rigid-body substructure S_k $(k = 1, 2, \ldots, n)$ with global Cartesian co-ordinate system O-xyz fixed in space, whereas C_k-$X_kY_kZ_k$ is a local co-ordinate system, parallel to O-xyz, fixed at the centre of gravity C_k of the substructure. The position of C_k relative to O is defined by the displacement vector $\mathbf{R}_{C_k}$ and the position vectors of the input $\mathbf{f}_{ki}$ $(i = 1, 2, \ldots, r_k)$ and output $\mathbf{f}_{(k+1)j}$ $(j = 1,2, \ldots, r_{(k+1)})$ force vectors are defined by $\boldsymbol{\rho}_{ki}$ and $\boldsymbol{\rho}_{(k+1)j}$, respectively, in the local co-ordinate system relative to C_k.

For a steady state sinusoidal excitation $e^{j\omega t}$, it follows from rigid-body dynamics theory [31] that the motion of this substructure S_k is described by the equations

$$m_k \ddot{\mathbf{R}}_{C_k} = j\omega m_k \mathbf{v}_{C_k} = \sum_{i=1}^{r_k} \mathbf{f}_{ki} + \sum_{l=1}^{r_{k+1}} \mathbf{f}_{(k+1)l}, \tag{1}$$

$$j\omega \mathbf{J}_k \cdot \boldsymbol{\Omega}_k = \sum_{i=1}^{r_k} \boldsymbol{\rho}_{ki} \times \mathbf{f}_{ki} + \sum_{l=1}^{r_{k+1}} \boldsymbol{\rho}_{(k+1)l} \times \mathbf{f}_{(k+1)l}, \tag{2}$$

where

$$\mathbf{J}_k = \begin{bmatrix} J_{xx}^k & -J_{xy}^k & -J_{xz}^k \\ -J_{yx}^k & J_{yy}^k & -J_{yz}^k \\ -J_{zx}^k & -J_{zy}^k & J_{zz}^k \end{bmatrix}$$

is the inertia matrix or inertia tensor defined with respect to C_k, m_k is the substructure's total mass, $\mathbf{v}_{C_k}$ and $\boldsymbol{\Omega}_k$ are velocity and angular velocity vectors, respectively, ω denotes the excitation frequency of the forces and $\mathrm{j} = \sqrt{-1}$.

From equations (1) and (2), one obtains

$$\mathbf{v}_{C_k} = \frac{1}{\mathrm{j}\omega m_k} \sum_{i=1}^{r_k} \mathbf{f}_{ki} + \frac{1}{\mathrm{j}\omega m_k} \sum_{l=1}^{r_{k+1}} \mathbf{f}_{(k+1)l},$$

$$= \frac{1}{\mathrm{j}\omega m_k} [\mathbf{I}, \mathbf{I}, \ldots, \mathbf{I}]_{r_k} \begin{Bmatrix} \mathbf{f}_{k1} \\ \mathbf{f}_{k2} \\ \vdots \\ \mathbf{f}_{kr_k} \end{Bmatrix} + \frac{1}{\mathrm{j}\omega m_k} [\mathbf{I}, \mathbf{I}, \ldots, \mathbf{I}]_{r_k} \begin{Bmatrix} \mathbf{f}_{(k+1)1} \\ \mathbf{f}_{(k+1)2} \\ \vdots \\ \mathbf{f}_{(k+1)r_{k+1}} \end{Bmatrix}, \tag{3}$$

$$\boldsymbol{\Omega}_k = \frac{1}{\mathrm{j}\omega} \mathbf{J}_k^{-1} \cdot \sum_{i=1}^{r_k} \boldsymbol{\rho}_{ki} \times \mathbf{f}_{ki} + \frac{1}{\mathrm{j}\omega} \mathbf{J}_k^{-1} \cdot \sum_{l=1}^{r_{k+1}} \boldsymbol{\rho}_{(k+1)l} \times \mathbf{f}_{(k+1)l}, \tag{4a}$$

where $\mathbf{I}$ is a unit tensor of the second order.

By simple vector manipulation, this last equation takes the form

$$\boldsymbol{\Omega}_k = \frac{1}{\mathrm{j}\omega} \sum_{i=1}^{r_k} (\mathbf{J}_k^{-1} \times \boldsymbol{\rho}_{ki}) \cdot \mathbf{f}_{ki} + \frac{1}{\mathrm{j}\omega} \sum_{l=1}^{r_{k+1}} (\mathbf{J}_k^{-1} \times \boldsymbol{\rho}_{(k+1)i}) \cdot \mathbf{f}_{(k+1)l}, \tag{4b}$$

or in matrix form

$$\boldsymbol{\Omega}_k = \frac{1}{\mathrm{j}\omega} \{\mathbf{J}_k^{-1} \times [\boldsymbol{\rho}_{k1}, \boldsymbol{\rho}_{k2}, \ldots, \boldsymbol{\rho}_{kr_k}]\} \cdot \begin{Bmatrix} \mathbf{f}_{k1} \\ \mathbf{f}_{k2} \\ \vdots \\ \mathbf{f}_{kr_k} \end{Bmatrix}$$

$$+ \frac{1}{\mathrm{j}\omega} \{\mathbf{J}_k^{-1} \times [\boldsymbol{\rho}_{(k+1)1}, \boldsymbol{\rho}_{(k+1)2}, \ldots, \boldsymbol{\rho}_{(k+1)r_{k+1}}]\} \cdot \begin{Bmatrix} \mathbf{f}_{(k+1)1} \\ \mathbf{f}_{(k+1)2} \\ \vdots \\ \mathbf{f}_{(k+1)r_{k+1}} \end{Bmatrix}. \tag{4c}$$

The velocity vectors at the input and output terminals of this substructure are

$$\mathbf{v}_{ki} = \mathbf{v}_{C_k} + \boldsymbol{\Omega}_k \times \boldsymbol{\rho}_{ki} \quad (i = 1, 2, \ldots, r_k), \tag{5}$$

$$\mathbf{v}_{(k+1)j} = \mathbf{v}_{C_k} + \boldsymbol{\Omega}_k \times \boldsymbol{\rho}_{(k+1)j} \quad (j = 1, 2, \ldots, r_{(k+1)}), \tag{6}$$

which in matrix form are given by

$$\begin{Bmatrix} \mathbf{v}_{k1} \\ \mathbf{v}_{k2} \\ \vdots \\ \mathbf{v}_{kr_k} \end{Bmatrix} = \begin{Bmatrix} \mathbf{I} \\ \mathbf{I} \\ \vdots \\ \mathbf{I} \end{Bmatrix}_{r_k} \cdot \mathbf{v}_{C_k} + \boldsymbol{\Omega}_k \times \begin{Bmatrix} \boldsymbol{\rho}_{k1} \\ \boldsymbol{\rho}_{k2} \\ \vdots \\ \boldsymbol{\rho}_{kr_k} \end{Bmatrix}, \tag{7}$$

$$\begin{Bmatrix} \mathbf{v}_{(k+1)1} \\ \mathbf{v}_{(k+1)2} \\ \vdots \\ \mathbf{v}_{(k+1)r_{k+1}} \end{Bmatrix} = \begin{Bmatrix} \mathbf{I} \\ \mathbf{I} \\ \vdots \\ \mathbf{I} \end{Bmatrix}_{r_{k+1}} \cdot \mathbf{v}_{C_k} + \boldsymbol{\Omega}_k \times \begin{Bmatrix} \boldsymbol{\rho}_{(k+1)1} \\ \boldsymbol{\rho}_{(k+1)2} \\ \vdots \\ \boldsymbol{\rho}_{(k+1)r_{k+1}} \end{Bmatrix}. \tag{8}$$

Substituting equations (3) and (4c) into equation (7) and applying the commutative law for vector products yields

$$\begin{aligned} \begin{Bmatrix} \mathbf{v}_{k1} \\ \mathbf{v}_{k2} \\ \vdots \\ \mathbf{v}_{kr_k} \end{Bmatrix} &= \frac{1}{\mathrm{j}\omega m_k} \begin{Bmatrix} \mathbf{I} \\ \mathbf{I} \\ \vdots \\ \mathbf{I} \end{Bmatrix}_{r_k} \cdot [\mathbf{I}, \mathbf{I}, \ldots, \mathbf{I}]_{r_k} \cdot \begin{Bmatrix} \mathbf{f}_{k1} \\ \mathbf{f}_{k2} \\ \vdots \\ \mathbf{f}_{kr_k} \end{Bmatrix} \\ &\quad + \frac{1}{\mathrm{j}\omega m_k} \begin{Bmatrix} \mathbf{I} \\ \mathbf{I} \\ \vdots \\ \mathbf{I} \end{Bmatrix}_{r_k} \cdot [\mathbf{I}, \mathbf{I}, \ldots, \mathbf{I}]_{r_{k+1}} \cdot \begin{Bmatrix} \mathbf{f}_{(k+1)1} \\ \mathbf{f}_{(k+1)2} \\ \vdots \\ \mathbf{f}_{(k+1)r_{k+1}} \end{Bmatrix} \\ &\quad - \frac{1}{\mathrm{j}\omega} \begin{Bmatrix} \boldsymbol{\rho}_{k1} \\ \boldsymbol{\rho}_{k2} \\ \vdots \\ \boldsymbol{\rho}_{kr_k} \end{Bmatrix} \times \left\{ \mathbf{J}_k^{-1} \times [\boldsymbol{\rho}_{k1}, \boldsymbol{\rho}_{k2}, \ldots, \boldsymbol{\rho}_{kr_k}] \right\} \cdot \begin{Bmatrix} \mathbf{f}_{k1} \\ \mathbf{f}_{k2} \\ \vdots \\ \mathbf{f}_{kr_k} \end{Bmatrix} \\ &\quad - \frac{1}{\mathrm{j}\omega} \begin{Bmatrix} \boldsymbol{\rho}_{k1} \\ \boldsymbol{\rho}_{k2} \\ \vdots \\ \boldsymbol{\rho}_{kr_k} \end{Bmatrix} \times \left\{ \mathbf{J}_k^{-1} \times [\boldsymbol{\rho}_{(k+1)1}, \boldsymbol{\rho}_{(k+1)2}, \ldots, \boldsymbol{\rho}_{(k+1)r_{k+1}}] \right\} \cdot \begin{Bmatrix} \mathbf{f}_{(k+1)1} \\ \mathbf{f}_{(k+1)2} \\ \vdots \\ \mathbf{f}_{(k+1)r_{k+1}} \end{Bmatrix}, \end{aligned} \tag{9}$$

which can be rewritten in the more compact form

$$\begin{aligned} \mathbf{V}_k &= \frac{1}{\mathrm{j}\omega} \left\{ m_k^{-1} \cdot \begin{Bmatrix} \mathbf{I} \\ \mathbf{I} \\ \vdots \\ \mathbf{I} \end{Bmatrix}_{r_k} \cdot [\mathbf{I}, \mathbf{I}, \ldots, \mathbf{I}]_{r_k} - \begin{Bmatrix} \boldsymbol{\rho}_{k1} \\ \boldsymbol{\rho}_{k2} \\ \vdots \\ \boldsymbol{\rho}_{kr_k} \end{Bmatrix} \times \mathbf{J}_k^{-1} \times [\boldsymbol{\rho}_{k1}, \boldsymbol{\rho}_{k2}, \ldots, \boldsymbol{\rho}_{kr_k}] \right\} \cdot \mathbf{F}_k \\ &\quad + \frac{1}{\mathrm{j}\omega} \left\{ m_k^{-1} \cdot \begin{Bmatrix} \mathbf{I} \\ \mathbf{I} \\ \vdots \\ \mathbf{I} \end{Bmatrix}_{r_k} \cdot [\mathbf{I}, \mathbf{I}, \ldots, \mathbf{I}]_{r_k} - \begin{Bmatrix} \boldsymbol{\rho}_{k1} \\ \boldsymbol{\rho}_{k2} \\ \vdots \\ \boldsymbol{\rho}_{kr_k} \end{Bmatrix} \right. \\ &\quad \left. \times \mathbf{J}_k^{-1} \times [\boldsymbol{\rho}_{(k+1)1}, \boldsymbol{\rho}_{(k+1)2}, \ldots, \boldsymbol{\rho}_{(k+1)r_{k+1}}] \right\} \cdot \mathbf{F}_{k+1}. \end{aligned} \tag{10}$$

Similarly, the velocity response at the output terminal of the substructure S_k becomes

$$\mathbf{V}_{k+1} = \frac{1}{\mathrm{j}\omega}\left\{ m_k^{-1} \cdot \begin{Bmatrix} \mathbf{I} \\ \mathbf{I} \\ \vdots \\ \mathbf{I} \end{Bmatrix}_{r_{k+1}} \cdot [\mathbf{I}, \mathbf{I}, \ldots, \mathbf{I}]_{r_{k+1}} - \begin{Bmatrix} \boldsymbol{\rho}_{(k+1)1} \\ \boldsymbol{\rho}_{(k+1)2} \\ \vdots \\ \boldsymbol{\rho}_{(k+1)r_{k+1}} \end{Bmatrix} \times \mathbf{J}_k^{-1} \times [\boldsymbol{\rho}_{k1}, \boldsymbol{\rho}_{k2}, \ldots, \boldsymbol{\rho}_{kr_k}] \right\} \cdot \mathbf{F}_k$$

$$+ \frac{1}{\mathrm{j}\omega}\left\{ m_k^{-1} \cdot \begin{Bmatrix} \mathbf{I} \\ \mathbf{I} \\ \vdots \\ \mathbf{I} \end{Bmatrix}_{r_{k+1}} \cdot [\mathbf{I}, \mathbf{I}, \ldots, \mathbf{I}]_{r_{k+1}} \right.$$

$$\left. - \begin{Bmatrix} \boldsymbol{\rho}_{(k+1)1} \\ \boldsymbol{\rho}_{(k+1)2} \\ \vdots \\ \boldsymbol{\rho}_{(k+1)r_{k+1}} \end{Bmatrix} \times \mathbf{J}_k^{-1} \times [\boldsymbol{\rho}_{(k+1)1}, \boldsymbol{\rho}_{(k+1)2}, \cdots, \boldsymbol{\rho}_{(k+1)r_{k+1}}] \right\} \cdot \mathbf{F}_{k+1}. \tag{11}$$

Equations (10) and (11) can now be expressed in the mobility matrix form

$$\begin{Bmatrix} \mathbf{V}_k \\ \mathbf{V}_{k+1} \end{Bmatrix} = \mathbf{M}_k \cdot \begin{Bmatrix} \mathbf{F}_k \\ \mathbf{F}_{k+1} \end{Bmatrix} = \begin{bmatrix} \mathbf{m}_{11}^{(k)} & \mathbf{m}_{12}^{(k)} \\ \mathbf{m}_{21}^{(k)} & \mathbf{m}_{22}^{(k)} \end{bmatrix} \cdot \begin{Bmatrix} \mathbf{F}_k \\ \mathbf{F}_{k+1} \end{Bmatrix}, \quad (k = 1, 2, \ldots, n), \tag{12}$$

where the sub-matrices $\mathbf{m}_{ij}^{(k)}$ $(i, j = 1, 2)$ are the mobility influence coefficient matrices in tensor form and are defined as follows:

$$\mathbf{m}_{11}^{(k)} = \frac{1}{\mathrm{j}\omega}\left\{ m_k^{-1} \cdot \begin{Bmatrix} \mathbf{I} \\ \mathbf{I} \\ \vdots \\ \mathbf{I} \end{Bmatrix}_{r_k} \cdot [\mathbf{I}, \mathbf{I}, \ldots, \mathbf{I}]_{r_k} - \begin{Bmatrix} \boldsymbol{\rho}_{k1} \\ \boldsymbol{\rho}_{k2} \\ \vdots \\ \boldsymbol{\rho}_{kr_k} \end{Bmatrix} \times \mathbf{J}_k^{-1} \times [\boldsymbol{\rho}_{k1}, \boldsymbol{\rho}_{k2}, \ldots, \boldsymbol{\rho}_{kr_k}] \right\}, \tag{13a}$$

$$\mathbf{m}_{12}^{(k)} = \frac{1}{\mathrm{j}\omega}\left\{ m_k^{-1} \cdot \begin{Bmatrix} \mathbf{I} \\ \mathbf{I} \\ \vdots \\ \mathbf{I} \end{Bmatrix}_{r_k} \cdot [\mathbf{I}, \mathbf{I}, \ldots, \mathbf{I}]_{r_{k+1}} - \begin{Bmatrix} \boldsymbol{\rho}_{k1} \\ \boldsymbol{\rho}_{k2} \\ \vdots \\ \boldsymbol{\rho}_{kr_k} \end{Bmatrix} \times \mathbf{J}_k^{-1} \times [\boldsymbol{\rho}_{(k+1)1}, \boldsymbol{\rho}_{(k+1)2}, \cdots, \boldsymbol{\rho}_{(k+1)r_{k+1}}] \right\},$$

(13b)

$$\mathbf{m}_{21}^{(k)} = \frac{1}{\mathrm{j}\omega}\left\{ m_k^{-1} \cdot \begin{Bmatrix} \mathbf{I} \\ \mathbf{I} \\ \vdots \\ \mathbf{I} \end{Bmatrix}_{r_{k+1}} \cdot [\mathbf{I}, \mathbf{I}, \ldots, \mathbf{I}]_{r_k} - \begin{Bmatrix} \boldsymbol{\rho}_{(k+1)1} \\ \boldsymbol{\rho}_{(k+1)2} \\ \vdots \\ \boldsymbol{\rho}_{(k+1)r_{k+1}} \end{Bmatrix} \times \mathbf{J}_k^{-1} \times [\boldsymbol{\rho}_{k1}, \boldsymbol{\rho}_{k2}, \ldots, \boldsymbol{\rho}_{kr_k}] \right\}, \quad (13c)$$

$$\mathbf{m}_{22}^{(k)} = \frac{1}{\mathrm{j}\omega}\left\{ m_k^{-1} \cdot \begin{Bmatrix} \mathbf{I} \\ \mathbf{I} \\ \vdots \\ \mathbf{I} \end{Bmatrix}_{r_{k+1}} \cdot [\mathbf{I}, \mathbf{I}, \ldots, \mathbf{I}]_{r_{k+1}} - \begin{Bmatrix} \boldsymbol{\rho}_{(k+1)1} \\ \boldsymbol{\rho}_{(k+1)2} \\ \vdots \\ \boldsymbol{\rho}_{(k+1)r_{k+1}} \end{Bmatrix} \times \mathbf{J}_k^{-1} \times [\boldsymbol{\rho}_{(k+1)1}, \boldsymbol{\rho}_{(k+1)2}, \ldots, \boldsymbol{\rho}_{(k+1)r_{k+1}}] \right\}. \quad (13d)$$

The impedance matrix $\mathbf{Z}_k$ is obtained by an inverse transformation of the mobility matrix $\mathbf{M}_k$: i.e. $\mathbf{Z}_k = \mathbf{M}_k^{-1}$. Thus for the kth substructure, it follows from equation (12) that the dynamic equation expressed in its impedance matrix form is given by

$$\begin{Bmatrix} \mathbf{F}_k \\ \mathbf{F}_{k+1} \end{Bmatrix} = \mathbf{Z}_k \cdot \begin{Bmatrix} \mathbf{V}_k \\ \mathbf{V}_{k+1} \end{Bmatrix} = \begin{bmatrix} \mathbf{z}_{11}^{(k)} & \mathbf{z}_{12}^{(k)} \\ \mathbf{z}_{21}^{(k)} & \mathbf{z}_{22}^{(k)} \end{bmatrix} \cdot \begin{Bmatrix} \mathbf{V}_k \\ \mathbf{V}_{k+1} \end{Bmatrix}, \quad (k = 1, 2, \ldots, n). \quad (14)$$

3.2. FLEXIBLE SUBSTRUCTURES

The mobility matrix describing the dynamics of a general three-dimensional elastic substructure S_k can be derived by adopting a modal analysis approach. Based on the assumption of a linear system with proportional damping, according to Thomson [32] the displacement vector $\mathbf{u}(\mathbf{R}, t)$ at position $\mathbf{R}$ of the elastic substructure can be expressed in terms of a mode shape vector matrix $\boldsymbol{\Phi}(\mathbf{R}) = [\boldsymbol{\varphi}_1, \boldsymbol{\varphi}_2, \ldots, \boldsymbol{\varphi}_p]$ and a generalized co-ordinate vector $\mathbf{q}(t) = [q_1, q_2, \ldots, q_p]^{\mathrm{T}}$ as

$$\mathbf{u}(\mathbf{R}, t) = \boldsymbol{\Phi}\mathbf{q}, \quad (15)$$

where $\boldsymbol{\varphi}_i (i = 1, 2, \ldots, p)$ is the ith mode shape vector function of the space co-ordinate vector $\mathbf{R} = [x, y, z]^{\mathrm{T}}$, and $q_i(t)$ is the generalized co-ordinate, corresponding to the ith mode shape vector function $\boldsymbol{\varphi}_i$. The velocity of the substructure is

$$\mathbf{v}(\mathbf{R}, t) = \dot{\mathbf{u}}(\mathbf{R}, t) = \boldsymbol{\Phi}\dot{\mathbf{q}} = \mathrm{j}\omega\boldsymbol{\Phi}\mathbf{q}. \quad (16)$$

From equation (16), the velocity vector $\mathbf{V}_k = \{\mathbf{v}_{k1}, \ldots, \mathbf{v}_{kj}, \ldots, \mathbf{v}_{kr_k}\}^{\mathrm{T}}$ at the input points $\mathbf{R}_{ki}$ and the velocity vector $\mathbf{V}_{k+1} = \{\mathbf{v}_{(k+1)1}, \ldots, \mathbf{v}_{(k+1)j}, \ldots, \mathbf{v}_{(k+1)r_{k+1}}\}^{\mathrm{T}}$ at the output points $\mathbf{R}_{(k+1)i}$ are denoted by

$$\mathbf{v}_{ki} = \mathrm{j}\omega\boldsymbol{\Phi}(\mathbf{R}_{ki})\mathbf{q}, \quad (i = 1, 2, \ldots, r_k),$$

$$\mathbf{v}_{(k+1)i} = \mathrm{j}\omega\boldsymbol{\Phi}(\mathbf{R}_{(k+1)i})\mathbf{q}, \quad (i = 1, 2, \ldots, r_{k+1}), \quad (17)$$

which can be rewritten in the matrix form as

$$\begin{Bmatrix} \mathbf{V}_k \\ \mathbf{V}_{k+1} \end{Bmatrix} = \mathrm{j}\omega \begin{Bmatrix} \mathbf{\Phi}(\mathbf{R}_{ki}) \\ \mathbf{\Phi}(\mathbf{R}_{(k+1)i}) \end{Bmatrix} \mathbf{q}. \tag{18}$$

For the three-dimensional elastic substructure S_k, it can be shown [31,32] that its generalized co-ordinate vector $\mathbf{q}$ satisfies the equation

$$\mathbf{M}(\mathbf{\Omega}^2 - \mathbf{I}_p\omega^2 + 2\mathrm{j}\xi\mathbf{\Omega}\omega)\mathbf{q} = [\mathbf{\Phi}^{\mathrm{T}}(\mathbf{R}_{ki}), \mathbf{\Phi}^{\mathrm{T}}(\mathbf{R}_{(k+1)i})] \cdot \begin{Bmatrix} \mathbf{F}_k \\ \mathbf{F}_{k+1} \end{Bmatrix}, \tag{19}$$

where $\mathbf{M}$ denotes the diagonal matrix of modal mass, $\mathbf{I}_p$ a unit matrix of p dimensions, $\mathbf{\Omega}$ the diagonal matrix of the natural frequencies of the substructure with free–free interface conditions, and $\xi = \mathrm{diag}(\xi_1, \xi_1, \ldots, \xi_p)$, the matrix of modal damping coefficients. The generalized co-ordinate vector $\mathbf{q}$ is now simply given by the expression

$$\mathbf{q} = (\mathbf{\Omega}^2 - \mathbf{I}_p\omega^2 + 2\mathrm{j}\xi\mathbf{\Omega}\omega)^{-1}\mathbf{M}^{-1}[\mathbf{\Phi}^{\mathrm{T}}(\mathbf{R}_{ki}), \mathbf{\Phi}^{\mathrm{T}}(\mathbf{R}_{(k+1)i})] \cdot \begin{Bmatrix} \mathbf{F}_k \\ \mathbf{F}_{k+1} \end{Bmatrix}. \tag{20}$$

The substitution of equation (20) into equation (18) yields

$$\begin{Bmatrix} \mathbf{V}_k \\ \mathbf{V}_{k+1} \end{Bmatrix} = \mathrm{j}\omega \begin{Bmatrix} \mathbf{\Phi}(\mathbf{R}_{ki}) \\ \mathbf{\Phi}(\mathbf{R}_{(k+1)i}) \end{Bmatrix} \mathbf{\Psi}_p [\mathbf{\Phi}^{\mathrm{T}}(\mathbf{R}_{ki}), \mathbf{\Phi}^{\mathrm{T}}(\mathbf{R}_{(k+1)i})] \cdot \begin{Bmatrix} \mathbf{F}_k \\ \mathbf{F}_{k+1} \end{Bmatrix}, \tag{21}$$

where $\mathbf{\Psi}_p = (\mathbf{\Omega}^2 - \mathbf{I}_p\omega^2 + 2\mathrm{j}\xi\mathbf{\Omega}\omega)^{-1}\mathbf{M}^{-1}$.

Thus, the unified dynamic equation for any substructure S_k presented in terms of the generalized mobility matrix $\mathbf{M}_k$, is given by

$$\begin{Bmatrix} \mathbf{V}_k \\ \mathbf{V}_{k+1} \end{Bmatrix} = \begin{bmatrix} \mathbf{m}_{11}^{(k)} & \mathbf{m}_{12}^{(k)} \\ \mathbf{m}_{21}^{(k)} & \mathbf{m}_{22}^{(k)} \end{bmatrix} \cdot \begin{Bmatrix} \mathbf{F}_k \\ \mathbf{F}_{k+1} \end{Bmatrix}, \quad (k = 1, 2, \ldots, n), \tag{22}$$

where

$$\mathbf{m}_{11}^{(k)} = \mathrm{j}\omega\mathbf{\Phi}(\mathbf{R}_{ki})\mathbf{\Psi}_p\mathbf{\Phi}^{\mathrm{T}}(\mathbf{R}_{ki}), \quad \mathbf{m}_{12}^{(k)} = \mathrm{j}\omega\mathbf{\Phi}(\mathbf{R}_{ki})\mathbf{\Psi}_p\mathbf{\Phi}^{\mathrm{T}}(\mathbf{R}_{(k+1)i}),$$

$$\mathbf{m}_{21}^{(k)} = \mathrm{j}\omega\mathbf{\Phi}(\mathbf{R}_{(k+1)i})\mathbf{\Psi}_p\mathbf{\Phi}^{\mathrm{T}}(\mathbf{R}_{ki}), \quad \mathbf{m}_{22}^{(k)} = \mathrm{j}\omega\mathbf{\Phi}(\mathbf{R}_{(k+1)i})\mathbf{\Psi}_p\mathbf{\Phi}^{\mathrm{T}}(\mathbf{R}_{(k+1)i}), \quad (k = 1, 2, \ldots, n). \tag{23}$$

In practice, only a limited number of natural modes of the substructure are admitted in the calculation of the mobility matrices. The number of modes, p say, can be determined by applying mode reduction criteria derived from a substructure analysis [33].

4. A PROGRESSIVE METHOD USING EQUIVALENT MOBILITY MATRICES

The theoretical and analytical aims of this investigation are (i) to determine the interaction forces and the corresponding velocity responses on any interface between substructures of a complex multiple coupled dynamic system subject to various force vector and velocity vector excitations and (ii) to predict the vibrational power flow into and transmission through each interface of the substructures. These objectives are achieved through the development of equivalent mobility and velocity transmissibility matrices as now described.

An application of the mobility matrices derived for the types of substructures described in section 3 provides description of the required generalized mobility matrices for substructures of complex coupled systems with multiple interaction interfaces. In order to characterize the dynamic coupling effect between substructures in the system, an *equivalent mobility matrix* (EMM) and a *velocity transmissibility matrix* (VTM) are first introduced with their respective definitions, allowing a sequential or progressive approach to be formulated. In its present form, this method is suitable to solve problems described by Case 1: $\mathbf{F}_1 = \hat{\mathbf{F}}_1$, $\mathbf{V}_{n+1} = \hat{\mathbf{V}}_{n+1}$ and Case 2: $\mathbf{V}_1 = \hat{\mathbf{V}}_1$, $\mathbf{V}_{n+1} = \hat{\mathbf{V}}_{n+1}$. That is, the evaluation of the vibrational characteristics of the system subject to imposed generalized boundary excitation conditions. The progressive approach allows determination of internal forces and response velocities on interfaces between the substructures of complicated coupled systems, to predict the dynamic characteristics of the overall coupled system or subsystems consisting of several substructures and to provide an estimation of input and transmitted power flows between the substructures.

From previous discussions, it has been shown that the dynamic equations describing the dynamical characteristics of all substructures S_k $(k = 1, 2, \ldots, n)$ can be represented by the generalized mobility matrix expressions

$$\begin{Bmatrix} \mathbf{V}_1 \\ \mathbf{V}_2 \end{Bmatrix} = \begin{bmatrix} \mathbf{m}_{11}^{(1)} & \mathbf{m}_{12}^{(1)} \\ \mathbf{m}_{21}^{(1)} & \mathbf{m}_{22}^{(1)} \end{bmatrix} \cdot \begin{Bmatrix} \mathbf{F}_1 \\ \mathbf{F}_2 \end{Bmatrix}, \tag{24}$$

$$\begin{Bmatrix} \mathbf{V}_k \\ \mathbf{V}_{k+1} \end{Bmatrix} = \begin{bmatrix} \mathbf{m}_{11}^{(k)} & \mathbf{m}_{12}^{(k)} \\ \mathbf{m}_{21}^{(k)} & \mathbf{m}_{22}^{(k)} \end{bmatrix} \cdot \begin{Bmatrix} \mathbf{F}_k \\ \mathbf{F}_{k+1} \end{Bmatrix}, \tag{25}$$

$$\begin{Bmatrix} \mathbf{V}_{n-1} \\ \mathbf{V}_n \end{Bmatrix} = \begin{bmatrix} \mathbf{m}_{11}^{(n-1)} & \mathbf{m}_{12}^{(n-1)} \\ \mathbf{m}_{21}^{(n-1)} & \mathbf{m}_{22}^{(n-1)} \end{bmatrix} \cdot \begin{Bmatrix} \mathbf{F}_{n-1} \\ \mathbf{F}_n \end{Bmatrix}, \tag{26}$$

$$\begin{Bmatrix} \mathbf{V}_n \\ \mathbf{V}_{n+1} \end{Bmatrix} = \begin{bmatrix} \mathbf{m}_{11}^{(n)} & \mathbf{m}_{12}^{(n)} \\ \mathbf{m}_{21}^{(n)} & \mathbf{m}_{22}^{(n)} \end{bmatrix} \cdot \begin{Bmatrix} \mathbf{F}_n \\ \mathbf{F}_{n+1} \end{Bmatrix}. \tag{27}$$

From equation (27) for substructure S_n it follows that

$$\mathbf{F}_{n+1} = [\mathbf{m}_{22}^{(n)}]^{-1} \cdot \mathbf{V}_{n+1} - [\mathbf{m}_{22}^{(n)}]^{-1} \cdot \mathbf{m}_{21}^{(n)} \cdot \mathbf{F}_n, \tag{28}$$

$$\begin{aligned} \mathbf{V}_n &= \{\mathbf{m}_{11}^{(n)} - \mathbf{m}_{12}^{(n)} \cdot [\mathbf{m}_{22}^{(n)}]^{-1} \cdot \mathbf{m}_{21}^{(n)}\} \cdot \mathbf{F}_n + \mathbf{m}_{12}^{(n)} \cdot [\mathbf{m}_{22}^{(n)}]^{-1} \cdot \mathbf{V}_{n+1} \\ &= \mathbf{M}_{ne} \cdot \mathbf{F}_n + \mathbf{M}_{nv} \cdot \mathbf{V}_{n+1}, \end{aligned} \tag{29}$$

where

$$\mathbf{M}_{ne} = \{\mathbf{m}_{11}^{(n)} - \mathbf{m}_{12}^{(n)} \cdot [\mathbf{m}_{22}^{(n)}]^{-1} \cdot \mathbf{m}_{21}^{(n)}\}, \qquad \mathbf{M}_{nv} = \mathbf{m}_{12}^{(n)} \cdot [\mathbf{m}_{22}^{(n)}]^{-1}. \tag{30}$$

Substituting equation (29) into equation (26) for substructure S_{n-1} one can derive the following equations describing the coupling characteristics of two adjacent substructures S_n and S_{n-1}:

$$\mathbf{F}_n = [\mathbf{m}_{22}^{(n-1)} - \mathbf{M}_{ne}]^{-1} \cdot [\mathbf{M}_{nv} \cdot \mathbf{V}_{n+1} - \mathbf{m}_{21}^{(n-1)} \cdot \mathbf{F}_{n-1}], \tag{31}$$

$$\begin{aligned} \mathbf{V}_{n-1} &= \{\mathbf{m}_{11}^{(n-1)} - \mathbf{m}_{12}^{(n-1)} \cdot [\mathbf{m}_{22}^{(n-1)} - \mathbf{M}_{ne}]^{-1} \cdot \mathbf{m}_{21}^{(n-1)}\} \mathbf{F}_{n-1} \\ &\quad + \mathbf{m}_{12}^{(n-1)} \cdot [\mathbf{m}_{22}^{(n-1)} - \mathbf{M}_{ne}]^{-1} \cdot \mathbf{M}_{nv} \cdot \mathbf{V}_{n+1} \\ &= \mathbf{M}_{(n-1)e} \cdot \mathbf{F}_{n-1} + \mathbf{M}_{(n-1)v} \cdot \mathbf{M}_{nv} \cdot \mathbf{V}_{n+1}, \end{aligned} \tag{32}$$

where

$$\mathbf{M}_{(n-1)e} = \{\mathbf{m}_{11}^{(n-1)} - \mathbf{m}_{12}^{(n-1)} \cdot [\mathbf{m}_{22}^{(n-1)} - \mathbf{M}_{ne}]^{-1} \cdot \mathbf{m}_{21}^{(n-1)}\},$$

$$\mathbf{M}_{(n-1)v} = \mathbf{m}_{12}^{(n-1)} \cdot [\mathbf{m}_{22}^{(n-1)} - \mathbf{M}_{ne}]^{-1}. \tag{33}$$

The continuation of this procedure leads to the following progressive or sequential formulation characterizing a coupled global system consisting of substructures $S_1, S_2, \ldots, S_k, \ldots, S_n$. Namely,

$$\mathbf{V}_k = \mathbf{M}_{ke} \cdot \mathbf{F}_k + \mathbf{N}_{kv} \cdot \hat{\mathbf{V}}_{n+1},$$

$$\mathbf{F}_{k+1} = [\mathbf{M}_{(k+1)e} - \mathbf{m}_{22}^{(k)}]^{-1} \cdot \mathbf{m}_{21}^{(k)} \cdot \mathbf{F}_k + [\mathbf{m}_{22}^{(k)} - \mathbf{M}_{(k+1)e}]^{-1} \cdot \mathbf{N}_{(k+1)v} \cdot \hat{\mathbf{V}}_{n+1},$$

$$P_k = \tfrac{1}{2} \operatorname{Re}\{\mathbf{F}_k^{\mathrm{H}} \cdot \mathbf{V}_k\},$$

$$\mathbf{M}_{ke} = \mathbf{m}_{11}^{(k)} - \mathbf{m}_{12}^{(k)} \cdot [\mathbf{m}_{22}^{(k)} - \mathbf{M}_{(k+1)e}]^{-1} \cdot \mathbf{m}_{21}^{(k)},$$

$$\mathbf{N}_{kv} = \mathbf{M}_{kv} \cdot \mathbf{M}_{(k+1)v} \ldots \mathbf{M}_{nv},$$

$$\mathbf{M}_{kv} = \mathbf{m}_{12}^{(k)} \cdot [\mathbf{m}_{22}^{(k)} - \mathbf{M}_{(k+1)e}]^{-1}, \quad (k = 1, 2, \ldots, n),$$

$$\mathbf{M}_{(n+1)e} = \mathbf{0}, \tag{34}$$

where P_k denotes the power flow through any interface of the kth substructure, H the *Hermitian* transpose and $\mathbf{0}$ the zero matrix.

The matrix $\mathbf{M}_{ke}$ defines the *equivalent mobility matrix* (EMM) of substructure S_k coupled to subsystems $S_{k+1}, \ldots, S_n$ $(k = 1, 2, \ldots, n)$. Physically, this matrix represents the velocity response vector $\mathbf{V}_k$ at the input coupling interface of S_k in the global system excited by a unit coupling force vector $\mathbf{F}_k$ at the interface between S_{k-1} and S_k. The introduction of EMM allows characterization of the dynamic coupling relation between substructures and subsystems consisting of several substructures in the overall system.

The matrix $\mathbf{N}_{kv}$ defines the *velocity transmissibility matrix* (VTM) which represents the velocity response vector $\mathbf{V}_k$ produced by a unit velocity input $\hat{\mathbf{V}}_{n+1}$, and it reflects the effect of the boundary motion excitations $\hat{\mathbf{V}}_{n+1}$ upon substructure S_k $(k = 1, 2, \ldots, n)$.

As these expressions indicate, all inverse matrix processes do not involve any generalized matrix inverses introducing uniqueness requirements [30]; this contrasts significantly with the vectorial four-pole parameter method [28, 29]. The progressive approach described by equation (34) begins from the prescribed excitation force vector $\mathbf{F}_1$ for Case 1 or from the prescribed excitation velocity vector $\mathbf{V}_1$ for Case 2. It is a forward sequential or progressive process from $k = 1$ to n. Thus, the internal coupling force vector $\mathbf{F}_k$ and the velocity response vectors $\mathbf{V}_k$ $(k = 1, 2, \ldots, n)$ on any substructure interface of the system are determined systematically. Moreover, the power flow P_k through any interface between substructures within the complex coupled system is efficiently predicted, and this is both advantageous and beneficial when undertaking a power flow analysis in complex coupled systems.

5. A PROGRESSIVE METHOD USING EQUIVALENT IMPEDANCE MATRICES

The derivation process used previously can be directly applied to develop a progressive method, based on the equivalent impedance matrices of the substructures, for analysis of the

complex coupled dynamic systems subject to the boundary excitation conditions described in Case 3: $\mathbf{F}_1 = \hat{\mathbf{F}}_1$, $\mathbf{F}_{n+1} = \hat{\mathbf{F}}_{n+1}$ and Case 4: $\mathbf{V}_1 = \hat{\mathbf{V}}_1$, $\mathbf{F}_{n+1} = \hat{\mathbf{F}}_{n+1}$. This is described as follows.

For all the multiple coupled substructures S_k ($k = 1, 2, \ldots, n$), the equations describing their dynamic behaviour are represented by the generalized impedance matrices

$$\begin{Bmatrix} \mathbf{F}_1 \\ \mathbf{F}_2 \end{Bmatrix} = \begin{bmatrix} \mathbf{z}_{11}^{(1)} & \mathbf{z}_{12}^{(1)} \\ \mathbf{z}_{21}^{(1)} & \mathbf{z}_{22}^{(1)} \end{bmatrix} \cdot \begin{Bmatrix} \mathbf{V}_1 \\ \mathbf{V}_2 \end{Bmatrix}, \tag{35}$$

$$\vdots$$

$$\begin{Bmatrix} \mathbf{F}_k \\ \mathbf{F}_{k+1} \end{Bmatrix} = \begin{bmatrix} \mathbf{z}_{11}^{(k)} & \mathbf{z}_{12}^{(k)} \\ \mathbf{z}_{21}^{(k)} & \mathbf{z}_{22}^{(k)} \end{bmatrix} \cdot \begin{Bmatrix} \mathbf{V}_k \\ \mathbf{V}_{k+1} \end{Bmatrix}, \tag{36}$$

$$\vdots$$

$$\begin{Bmatrix} \mathbf{F}_n \\ \mathbf{F}_{n+1} \end{Bmatrix} = \begin{bmatrix} \mathbf{z}_{11}^{(n)} & \mathbf{z}_{12}^{(n)} \\ \mathbf{z}_{21}^{(n)} & \mathbf{z}_{22}^{(n)} \end{bmatrix} \cdot \begin{Bmatrix} \mathbf{V}_n \\ \mathbf{V}_{n+1} \end{Bmatrix} \tag{37}$$

as defined in equation (14). By repeating the analysis described in section 4, the impedance-based expressions describing the dynamics of the kth substructure are given by

$$\begin{aligned}
\mathbf{F}_k &= \mathbf{Z}_{ke} \cdot \mathbf{V}_k + \mathbf{T}_{kF} \cdot \hat{\mathbf{F}}_{n+1}, \\
\mathbf{V}_{k+1} &= [\mathbf{Z}_{(k+1)e} - \mathbf{z}_{22}^{(k)}]^{-1} \cdot \mathbf{z}_{21}^{(k)} \cdot \mathbf{V}_k + [\mathbf{z}_{22}^{(k)} - \mathbf{Z}_{(k+1)e}]^{-1} \cdot \mathbf{T}_{(k+1)F} \cdot \hat{\mathbf{F}}_{n+1}, \\
P_k &= \tfrac{1}{2} \operatorname{Re}\{\mathbf{F}_k^{\mathrm{H}} \cdot \mathbf{V}_k\}, \\
\mathbf{Z}_{ke} &= \mathbf{z}_{11}^{(k)} - \mathbf{z}_{12}^{(k)} \cdot [\mathbf{z}_{22}^{(k)} - \mathbf{Z}_{(k+1)e}]^{-1} \cdot \mathbf{z}_{21}^{(k)}, \\
\mathbf{T}_{kF} &= \mathbf{Z}_{kF} \cdot \mathbf{Z}_{(k+1)F} \cdots \mathbf{Z}_{nF}, \\
\mathbf{Z}_{kF} &= \mathbf{z}_{12}^{(k)} \cdot [\mathbf{z}_{22}^{(k)} - \mathbf{Z}_{(k+1)e}]^{-1}, \quad (k = 1, 2, \ldots, n), \\
\mathbf{Z}_{(n+1)e} &= \mathbf{0}.
\end{aligned} \tag{38}$$

The matrix $\mathbf{Z}_{ke}$ defines the *equivalent impedance matrix* (EIM) of substructure S_k coupled to subsystems $S_{k+1}, \ldots, S_n$ ($k = 1, 2, \ldots, n$). The matrix $\mathbf{T}_{kF}$ defines the *force transmissibility matrix* (FTM) which represents the force vector $\mathbf{F}_k$ produced by a unit dynamic input force $\hat{\mathbf{F}}_{n+1}$ exerted on the boundary of substructure S_n, and it represents the effect of the boundary force excitations upon substructure S_k ($k = 1, 2, \ldots, n$).

The introduction of EIM now allows the characterization of the dynamic coupling between substructures. The prediction process is similar to the one described in section 4. For example, the EIM approach commences from the prescribed excitation force vector $\mathbf{F}_1$ for Case 3 or from the prescribed excitation velocity vector $\mathbf{V}_1$ for Case 4 and progresses forward until substructure $k = n$ is reached. Again, the EIM progressive or sequential method provides another effective method to predict the power flow transmissions between substructures in complex coupled systems.

6. APPLICATION OF THE PROGRESSIVE METHOD TO A RAFT ISOLATION SYSTEM

6.1. MODEL OF RAFT ISOLATION SYSTEM

Various types of floating rafts have been installed in buildings, ships and offshore constructions as advanced isolation systems to provide better vibration and acoustic isolation effectiveness [22, 34–37]. A typical installation consists of one or several vibrating machines mounted via isolators onto a continuous floating raft structure supported by a series of resilient pads to a base structure. For example, Figure 3 shows a floating raft isolation system idealized by five substructures S_k ($k = 1, 2, \ldots, 5$). Substructure S_1 models two machines mounted through four isolators ($l = 1, 2, 3, 4$) grouped in twos in substructure S_2 with each isolator group supporting one machine. Theoretically, the number and distribution of components in each isolator group may vary and the isolator groups are thus not necessarily identical, but in practice, it is more usual for them to be so. These isolators are attached to a flexible raft S_3 of mass m_r and through N identical isolators in substructure S_4 to a flexible foundation S_5 of mass m_b. The two machines are treated as rigid bodies of masses m_1 and m_2 respectively. The dynamic characteristics of the isolator groups in substructure S_2 are idealized as spring–mass–spring systems with their complex stiffness $K_l^* = K_l\,(1 + \mathrm{j}\eta_l)$ and lumped masses M_l ($l = 1, 2, 3, 4$) located at the middle of each spring as shown in Figure 4. The raft S_3 is idealized by a free–free beam, with complex stiffness $E^* = E(1 + \mathrm{j}\delta\,)$ reflecting structural elasticity E and damping δ. Similarly, the N identical isolators form substructure S_4 in which each isolator is idealized as a lumped system consisting of a complex stiffness $K^* = K(1 + \mathrm{j}\eta)$, damping η and lumped mass M. The spring–mass–spring system shown in Figure 4 has two degrees of freedom for which the first natural frequency is zero representing its rigid motion and the second one equals the first natural frequency $\Omega_l^{(2)}$ of the elastic isolator fixed at its two ends. This model is used to describe the dynamic effect of the elastic isolator caused by its rigid motion and elastic deformation relative to its two ends. The non-zero lumped masses M_l ($l = 1, 2, 3, 4$) can be determined by the equation $\Omega_l^{(2)} = 2\sqrt{K_l/M_l}$. If the mass effect of an isolator is neglected, its stiffness matrix is singular and the correponding mobility matrix does not exist. For this approximation, the impedance method described in section 5 may be chosen. It is also noticed that the isolator mass is simply applied to the supporting panel in reference [20], and yet another approximation may be made as used in finite element formulations, i.e., attaching $\frac{1}{2}$ mass evenly to the two ends of the spring element of the stiffness K_l^*. The foundation is treated as an end clamped–clamped flexible beam and is also modelled by

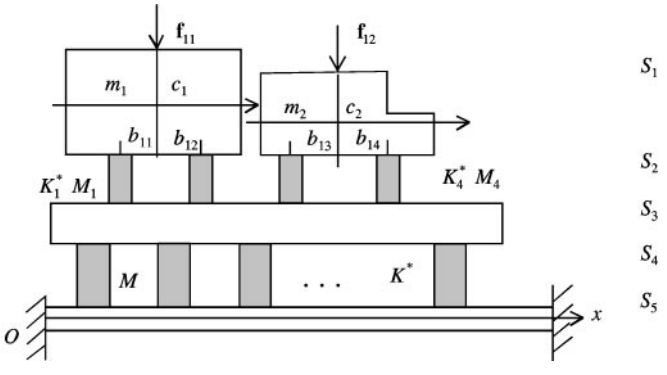

Figure 3. Flexible floating raft isolation system subject to multiple excitations.

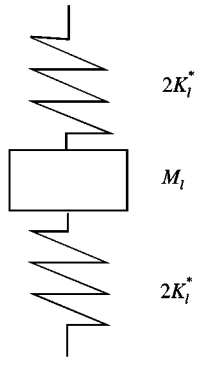

Figure 4. Idealized isolator model.

a complex-valued stiffness similar to substructure S_3. No particular requirements are imposed (i.e., symmetry) on the overall arrangement of the system.

6.2. MOBILITY MATRICES OF SUBSTRUCTURES

Applying the theory described in section 3, one obtains the mobility matrices for each substructure as follows.

For substructure S_1 with two inputs and four outputs, the generalized mobility matrix $\mathbf{M}_1$ is expressed as

$$\begin{Bmatrix} \mathbf{V}_{11} \\ \mathbf{V}_{12} \\ \cdots \\ \mathbf{V}_{21} \\ \mathbf{V}_{22} \\ \mathbf{V}_{23} \\ \mathbf{V}_{24} \end{Bmatrix} = \begin{bmatrix} \mathbf{m}_{11}^{(1)} & \mathbf{m}_{12}^{(1)} \\ \mathbf{m}_{21}^{(1)} & \mathbf{m}_{22}^{(1)} \end{bmatrix} \cdot \begin{Bmatrix} \mathbf{F}_{11} \\ \mathbf{F}_{12} \\ \cdots \\ \mathbf{F}_{21} \\ \mathbf{F}_{22} \\ \mathbf{F}_{23} \\ \mathbf{F}_{24} \end{Bmatrix} \tag{39}$$

and the sub-matrices of matrix $\mathbf{M}_1$ are given by

$$\mathbf{m}_{11}^{(1)} = \frac{1}{\mathrm{j}\omega}\begin{bmatrix} 1/m_1 & 0 \\ 0 & 1/m_2 \end{bmatrix}, \qquad \mathbf{m}_{12}^{(1)} = \frac{1}{\mathrm{j}\omega}\begin{bmatrix} 1/m_1 & 1/m_1 & 0 & 0 \\ 0 & 0 & 1/m_2 & 1/m_2 \end{bmatrix}, \qquad m_{21}^{(1)} = [m_{12}^{(1)}]^{\mathrm{T}}, \tag{40a–c}$$

where J_1 and J_2 denote the rotational inertia of each machine about its centre of gravity, respectively, and ω represents the frequency of excitations applied to the machines.

$$\mathbf{m}_{22}^{(1)} = \frac{1}{\mathrm{j}\omega}\begin{bmatrix} \begin{bmatrix} \dfrac{1}{m_1} + \dfrac{b_{11}^2}{J_1} & sym \\ \dfrac{1}{m_1} - \dfrac{b_{11}b_{12}}{J_1} & \dfrac{1}{m_1} + \dfrac{b_{11}^2}{J_1} \end{bmatrix} & \mathbf{0}_{2\times 2} \\ \mathbf{0}_{2\times 2} & \begin{bmatrix} \dfrac{1}{m_2} + \dfrac{b_{13}^2}{J_2} & sym \\ \dfrac{1}{m_2} - \dfrac{b_{13}b_{14}}{J_2} & \dfrac{1}{m_2} + \dfrac{b_{13}^2}{J_2} \end{bmatrix} \end{bmatrix}_{4\times 4}, \tag{40d}$$

For the isolator substructure S_2 consisting of four isolators ($l = 1, 2, 3, 4$), say, each idealized by the model shown in Figure 4, the generalized mobility matrix $\mathbf{M}_2$ is represented by

$$\mathbf{m}_{11}^{(2)} = \mathrm{diag}\left[\frac{\mathrm{j}\omega(4K_l^* - M_l\omega^2)(2K_l^* - M_l\omega^2)}{2K_l^*[(2K_l^* - M_l\omega^2)^2 - (2K_l^*)^2]}\right]_{4\times 4}, \tag{41a}$$

$$\mathbf{m}_{12}^{(2)} = \mathrm{diag}\left[\frac{\mathrm{j}\omega(4K_l^* - M_l\omega^2)}{[(2K_l^* - M_l\omega^2)^2 - (2K_l^*)^2]}\right]_{4\times 4} = \mathbf{m}_{21}^{(2)}, \tag{41b}$$

$$\mathbf{m}_{22}^{(2)} = \mathbf{m}_{11}^{(2)}. \tag{41c}$$

Similarly, for the N isolators in substructure S_4, the sub-matrices of the generalized mobility matrix $\mathbf{M}_4$ are given by

$$\mathbf{m}_{11}^{(4)} = \alpha(2K^* - M\omega^2)\mathbf{I}_{N\times N} = \mathbf{m}_{22}^{(4)}, \tag{42a}$$

$$\mathbf{m}_{12}^{(4)} = 2K^*\alpha\ \mathbf{I}_{N\times N} = \mathbf{m}_{21}^{(4)}, \tag{42b}$$

where

$$\alpha = \frac{\mathrm{j}\omega(4K^* - M\omega^2)}{2K^*[(2K^* - M\omega^2)^2 - (2K^*)^2]}. \tag{42c}$$

For the flexible floating raft system S_3, the mobility matrix $\mathbf{M}_3$ can be derived by using the modal analysis method described in section 3. The sub-matrices of $\mathbf{M}_3$ are

$$\mathbf{m}_{11}^{(3)} = [\chi_{ls}(x_l^{(3)}, x_s^{(3)})]_{4\times 4}, \qquad \mathbf{m}_{12}^{(3)} = [\chi_{ls}(x_l^{(3)}, x_s^{(4)})]_{4\times N}, \tag{43a, b}$$

$$\mathbf{m}_{21}^{(3)} = [\chi_{ls}(x_l^{(4)}, x_s^{(3)})]_{N\times 4} = \mathbf{m}_{12}^{(3)\mathrm{T}}, \qquad \mathbf{m}_{22}^{(3)} = [\chi_{ls}(x_l^{(4)}, x_s^{(4)})]_{N\times N}, \tag{43c, d}$$

where

$$\chi_{ls}(x_l, x_s) = \frac{\mathrm{j}\omega}{m_r}\sum_{n=1}^{p}\frac{\varphi_n(x_l)\varphi_n(x_s)}{[\Omega_n^{(3)}]^2(1 + \mathrm{j}\delta) - \omega^2}. \tag{43e}$$

Here $x_l^{(3)}(l = 1, 2, 3, 4)$ denotes the position co-ordinates of the isolators in substructure S_2 mounted between the machines and the raft, and $x_s^{(4)}$ ($s = 1, 2, \ldots, N$) those in substructure S_4 mounted between the raft and the supporting structure. $\varphi_n(x)$ is the normal mode function of the free–free beam for the raft structure in S_3.

By following the same procedure, the mobility matrix for the supporting foundation S_5 can be described in the form

$$\mathbf{M}_5 = [\mathbf{m}_{sk}^{(5)}]_{N\times N}, \tag{44}$$

$$\mathbf{m}_{sk}^{(5)} = \frac{\mathrm{j}\omega}{m_b}\sum_{n=1}^{\infty}\frac{\psi_n(x_s^{(5)})\psi_n(x_k^{(5)})}{[\Omega_n^{(5)}]^2(1+\mathrm{j}\delta)-\omega^2}, \quad (s,k=1,2,\ldots,N), \tag{45}$$

where ψ_n denotes the normal mode function of the end clamped–clamped beam of the idealized supporting structure in S_5, and $x_s^{(5)}$ $(s=1,2,\ldots,N)$ represents the position co-ordinates of the isolators mounted on the supporting foundation. With all mobility matrices derived, we can now determine all the forces, velocity responses and power flow through the coupled interfaces of the system by applying the mobility progressive method.

6.3. PROGRESSIVE FORMULATIONS

For this demonstration of the progressive approach to the flexible raft isolation system shown in Figure 3, the prescribed excitation force vector $\mathbf{F}_1 = \{\mathbf{f}_{11}, \mathbf{f}_{12}\}^{\mathrm{T}}$, and a clamped boundary condition is imposed on substructure S_5, i.e. $\hat{\mathbf{V}}_6 = \mathbf{0}$. For this reason, the mobility-based approach method is used, as discussed in section 4. For illustration purposes and as a special example of Case 1, it follows that $n=5$ and $\hat{\mathbf{V}}_{n+1} = \mathbf{0}$ in equation (34), and the mobility progressive formulations reduce to the form

$$\begin{aligned}
\mathbf{V}_k &= \mathbf{M}_{ke}\cdot\mathbf{F}_k,\\
\mathbf{F}_{k+1} &= [\mathbf{M}_{(k+1)e} - \mathbf{m}_{22}^{(k)}]^{-1}\cdot\mathbf{m}_{21}^{(k)}\mathbf{F}_k,\\
P_k &= \tfrac{1}{2}\,\mathrm{Re}\{\mathbf{F}_k^{\mathrm{H}}\cdot\mathbf{M}_{ke}\cdot\mathbf{F}_k\},\\
\mathbf{M}_{ke} &= \mathbf{m}_{11}^{(k)} + \mathbf{m}_{12}^{(k)}\cdot[\mathbf{M}_{(k+1)e} - \mathbf{m}_{22}^{(k)}]^{-1}\cdot\mathbf{m}_{21}^{(k)}, \quad (k=1,2,\ldots,5),\\
\mathbf{M}_{ke} &= \mathbf{0},
\end{aligned} \tag{46}$$

6.4. NUMERICAL RESULTS

In designing raft isolation systems, estimation of the total power flow transmitted to the foundation is of ultimate importance. This is often used as the cost function minimized to assess vibration control [20, 21, 38, 39]. Therefore, the transmitted forces $\mathbf{F}_5$ and velocity responses $\mathbf{V}_5$ at the N mounting points as well as the total power flow P_5 transmitted to the supporting foundation through the N anti-vibration mountings are presented here to illustrate the dynamic characteristics of the chosen floating raft vibration isolation system.

For simplicity of calculations and to illustrate the mobility-based approach, one can consider only vertical harmonic excitation forces of the forms $f_{11} = \mathrm{e}^{\mathrm{j}\omega t}$, $\lambda = f_{12}/f_{11} = 2$. In the subsequent calculations the following data are used: $m_1 = m_2 = 2500$ kg, $J_1 = J_2 = 414{\cdot}6$ m^4, $b_{ij} = 1$ m $(i,j=1,2)$; $K_l = 1{\cdot}67$ MN/m, $M_l = 0$, $\eta_l = 0{\cdot}3$ $(l=1,2,3,4)$; $K = 4{\cdot}12$ MN/m, $M = 0$, $\eta = 0{\cdot}2$, $N = 4$; $m_b = 1250$ kg; density of both beams $\rho = 7850$ kg/m^3 and Young's modulus $E = 2{\cdot}07\times10^{11}$ N/m^2, damping $\delta = 0{\cdot}05$. For the flexible beams, the first 30 natural modes (i.e., $p=30$) are admitted into the power flow calculations. (Such a number is used only to illustrate the applicability of the approach and

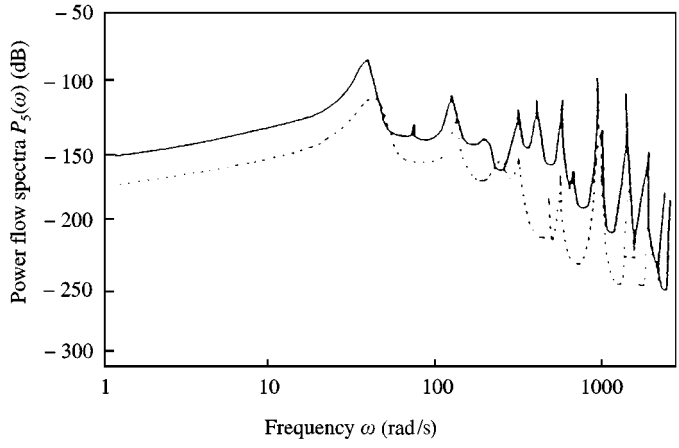

Figure 5. Power flow spectra influenced by the stiffness of the raft structure in substructure S_3: ——, $\Omega_1^{(3)} = 70$ rad/s; - - - -, $\Omega_1^{(3)} = 169$ rad/s.

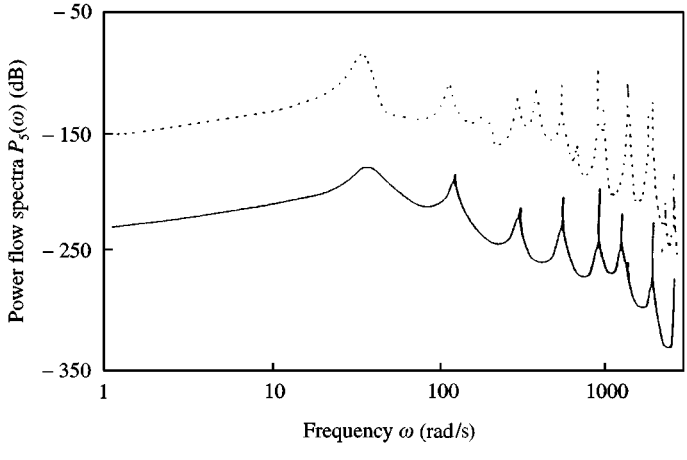

Figure 6. Comparison of $P_5(\omega)$ for $\Omega_1^{(3)} = 70$ (- - - -) and 1200 rad/s (——).

questions of sensitivity of mathematical modelling, accuracy, etc., are excluded from this study.) The power flow spectra are expressed in decibel scale (dB reference: 10^{-12} W). To examine the effect of the floating raft stiffness on power flows, three different fundamental frequencies: $\Omega_1^{(3)} = 70$, 169, 1200 rad/s, of the floating raft are considered.

The variations of the power flow spectra with changes of the free–free flexible beam raft's fundamental frequency $\Omega_1^{(3)}$are shown in Figures 5 and 6. It is observed from these two figures that when $\Omega_1^{(3)}$ becomes relatively high significant reduction in the power flow transmission can be achieved. This evidence indicates that an increase in the frequency $\Omega_1^{(3)}$/(dynamic stiffness of the raft) causes a reduction of the power transmitted to the foundation, thus providing good vibration isolation. Therefore, to obtain good vibration isolation and control, it might be prudent to increase the stiffness of the raft structures.

Figure 7 shows a comparison of the input power spectrum $P_1(\omega)$ by the two machine-generated excitations in substructure S_1 to the total power flow transmission spectrum $P_5(\omega)$. The difference between them indicates the energy dissipated in this raft isolation system. It is seen that the input power flow spectrum $P_1(\omega)$ is relatively simple in

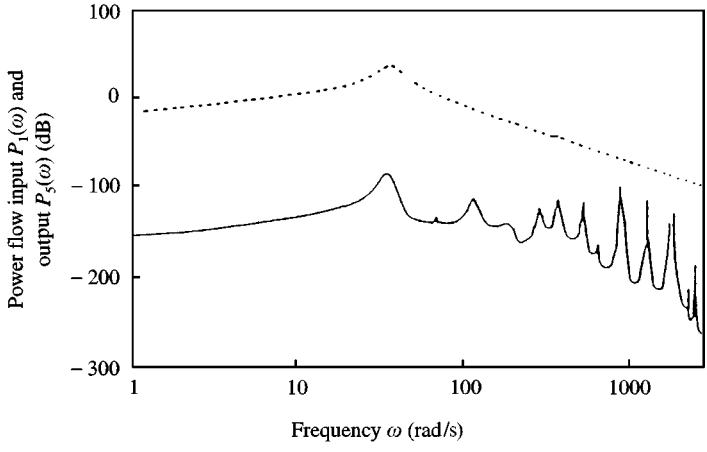

Figure 7. Comparison of input power flow spectrum $P_1(\omega)$ (- - - -) with output $P_5(\omega)$ (——).

form with one pronounced peak, whereas the transmission spectrum $P_5(\omega)$ varies significantly with the exciting frequencies, since it now contains contributions from the coupled dynamics of the overall system. This indicates that the total input power is less sensitive than the total output power to changes in the excitation frequencies. The power flow transmission behaviour revealed from these numerical results is supported by experimental observations and measurements [40, 41].

7. CONCLUSIONS

The generalized mobility/impedance matrices of a three-dimensional rigid/elastic structure with various configurations are derived, which can be used extensively in the dynamical analysis of a wide range of practical problems in engineering. The *equivalent mobility matrix* (EMM) and *equivalent impedance matrix* (EIM) methods introduced in this paper provide powerful techniques to describe the dynamical coupling interaction mechanisms between substructures or a subsystem assembled from several inter-connected substructures within the overall system. Based on these two proposed matrices, two progressive or sequential approaches are developed to predict the force vectors and velocity response vectors as well as the power flows at interfaces between substructures in complex coupled systems. The example of a flexible raft vibration isolation system demonstrates the application of the proposed generalized approaches.

The two mathematical models developed herein have the following attributes.

(1) They apply to practical engineering problems requiring prescribed force and/or velocity boundary conditions. Namely, boundary value problems relating to the following conditions: (a) $\mathbf{F}_1 = \hat{\mathbf{F}}_1$, $\mathbf{V}_{n+1} = \hat{\mathbf{V}}_{n+1}$; (b) $\mathbf{V}_1 = \hat{\mathbf{V}}_1$, $\mathbf{V}_{n+1} = \hat{\mathbf{V}}_{n+1}$; (c) $\mathbf{F}_1 = \hat{\mathbf{F}}_1$, $\mathbf{F}_{n+1} = \hat{\mathbf{F}}_{n+1}$; (d) $\mathbf{V}_1 = \hat{\mathbf{V}}_1$, $\mathbf{F}_{n+1} = \hat{\mathbf{F}}_{n+1}$.

(2) The system studied herein consists of various substructures, rigid or flexible, as well as more general configurations. For the special case of periodic systems, where the substructures are identical and the mobility or impedance matrices of substructures are similar, these methods therefore become even more effective.

(3) Multiple excitations and multiple coupled interfaces are considered in the mathematical model.

(4) The proposed progressive formulations use the normal inverse process of square matrices instead of the generalized inverse process of rectangular matrices when dealing with multi-input/multi-output (MIMO) systems [28, 29]. This provides benefits of simplification when applied to real designs of isolation systems and to the dynamic analysis of complex coupled systems.

(5) The proposed progressive approaches are systematic in their implementation and are of a form readily transferable into computer code. They are also very efficient in reducing the complexity of a power flow analysis when applied to complex dynamic coupled systems.

(6) The approach is very conveniently extended if additional substructures are further connected to the original dynamic system, without involving much additional computational effort.

ACKNOWLEDGMENT

This research is partially supported by NSFC and NSF of Shandong Province. We express our deep appreciation to the Royal Society and China Scholarship Council for supporting Professor Y. P. Xiong's related research in the UK.

REFERENCES

1. R. H. LYON 1975 *Statistical Energy Analysis of Dynamic Systems*. Cambridge, MA: MIT Press.
2. W. G. PRICE and A. J. KEANE 1994 *Philosophical Transactions of the Royal Society of London* A **346**, 429–554. Statistical energy analysis.
3. A. J. KEANE and W. G. PRICE 1997 *A Statistical Energy Analysis*: *An Overview with Application in Structural Dynamics*. Cambridge: Cambridge University Press.
4. F. J. FAHY and W. G. PRICE (editors) 1999 *IUTAM Symposium on Statistical Energy Analysis*, AA Dordrecht: Kluwer Academic Publishers.
5. H. G. D. GOYDER and R. G. WHITE 1980 *Journal of Sound and Vibration* **68**, 59–75. Vibrational power flow from machines into buildup structures, Part I: introduction and approximate analysis of beam and plate-like foundations.
6. H. G. D. GOYDER and R. G. WHITE 1980 *Journal of Sound and Vibration* **68**, 77–96. Vibrational power flow from machines into buildup structures, Part II: wave propagation and power flow in beam-stiffened plates.
7. H. G. D. GOYDER and R. G. WHITE 1980 *Journal of Sound and Vibration* **68**, 97–117. Vibrational power flow from machines into buildup structures, Part III: power flow through isolation systems.
8. R. J. PINNINGTON and R. G. WHITE 1981 *Journal of Sound and Vibration* **75**, 179–197. Power flow through machine isolators to resonant and non-resonant beam.
9. R. J. PINNINGTON 1987 *Journal of Sound and Vibration* **166**, 515–530. Vibrational power flow transmission to a seating of a vibration isolated motor.
10. R. S. LANGLEY 1990 *Journal of Sound and Vibration* **136**, 439–452. Analysis of power flow in beams and frameworks using the direct-dynamic stiffness method.
11. B. L. CLARKSON 1991 *Journal of Mechanical Engineering Science*, Part C **205**, 17–22. Estimation of the coupling loss factor of structural joints.
12. D. J. MEAD, R. G. WHITE and X. M. ZHANG 1994 *Journal of Sound and Vibration* **169**, 558–561. Power transmission in a periodically supported infinite beam excited at a single point.
13. J. M. CUSCHIERI 1990 *Journal of Sound and Vibration* **143**, 65–74. Vibration transmission through periodic structures using a mobility power flow approach.
14. J. M. CUSCHIERI 1990 *Journal of the Acoustical Society of America* **87**, 1159–1165. Structural power flow analysis using a mobility approach in an L-shaped plate.
15. N. H. FARAG and J. PAN 1996 *Journal of Acoustical Society of America* **95**, 2930–2937.Dynamic response and power flow in two-dimensional coupled beam structures under in-plane loading.
16. R. S. MING, J. PAN and M. P. NORTON 1999 *Journal of the Acoustical Society of America* **105**, 1702–1713. The mobility functions and their application in calculating power flow in coupled cylindrical shells.

17. P. GARDONIO, S. J. ELLIOT and R. J. PINNINGTON 1997 *Journal of Sound and Vibration* **207**, 61–93. Active isolation of structural vibration on a multiple-degree-of-freedom system, Part I: the dynamics of the system.
18. P. GARDONIO, S. J. ELLIOT and R. J. PINNINGTON 1997 *Journal of Sound and Vibration* **207**, 95–121. Active isolation of structural vibration on a multiple-degree-of-freedom system, Part II: effectiveness of active control strategies.
19. P. E. CHO and R. J. BERNHARD 1998 *Journal of Sound and Vibration* **211**, 593–605. Energy flow analysis of coupled beams.
20. J. PAN, J. Q. PAN and C. H. HANSEN 1992 *Journal of the Acoustical Society of America* **92**, 895–907. Total power flow from a vibrating rigid body to a thin panel through multiple elastic mounts.
21. W. L. LI and P. LAVRICH 1999 *Journal of Sound and Vibration* **224**, 757–774. Prediction of power flows through machine vibration isolators.
22. T. Y. LI, X. M. ZHANG, Y. T. ZUO and M. B. XU 1997 *Journal of Sound and Vibration* **202**, 47–54. Structural power flow analysis for a floating raft isolation system consisting of constrained damped beams.
23. J. T. XING and W. G. PRICE 1999 *Proceedings of the Royal Society of London, Series A.* **455**, 401–436. A power-flow analysis based on continuum dynamics.
24. R. E. D. BISHOP and D. C. JOHNSON 1960 *The Mechanics of Vibration.* Cambridge: Cambridge University Press.
25. D. OTTE 1990 *Proceedings of the 8th International Modal Analysis Conference*, Vol. 1, 213–220. Coupling of structures using measured FRFs by means of SVD-based data reduction techniques.
26. C. T. MOLLY 1957 *Journal of the Acoustical Society of America* **29**, 842–853. Use of four-pole parameters in vibration calculations.
27. J. C. SNOWDON 1971 *Journal of Sound and Vibration* **15**, 307–323. Mechanical four-pole parameters and their applications.
28. J. Y. HA and K. J. KIM 1995 *Journal of Sound and Vibration* **180**, 333–350. Analysis of MIMO mechanical systems using the vectorial four pole parameter method.
29. Y. P. XIONG 1996 *Ph.D. Dissertation, Shandong University of Technology*. Power flow transmission mechanism and optimum control of complex coupled flexible system of machinery and foundation (in Chinese).
30. R. M. PRINGLE and A. A. RAYNER 1971 *Generalized Inverse Matrices with Applications to Statistics.* London: Charles Griffin & Company Limited.
31. J. L. MERIAM and L. G. KRAIGE 1998 *Engineering Mechanics, Dynamics.* New York: John Wiley & Sons, fourth edition.
32. W. T. THOMSON 1988 *Theory of Vibration with Applications.* Engle Wood Cliffs, NJ: Prentice-Hall, third edition.
33. J. T. XING, W. G. PRICE and Q. H. DU 1996 *Philosphical Transactions of the Royal Society of London Series A* **354**, 259–295. Mixed finite element substructure-subdomain methods for the dynamical analysis of coupled fluid-solid interaction problems.
34. A. C. NILSSON and B. SELAND 1977 *Proceedings of Inter-Noise* '77, 663–667. Floating floor on ship and offshore constructions.
35. J. Q. PAN and C. H. HABAEN 1994 *Journal of Vibration and Acoustics- Transactions of the ASME.* **116**, 496–505. Power transmission from a vibrating source through an intermediate flexible panel to a flexible cylinder.
36. Y. P. XIONG and K. J. SONG 1996 *Chinese Journal of Mechanical Engineering* **9**, 260–264. Power flow analysis for a new isolation system—flexible floating raft.
37. Y. P. XIONG 1996 *Chinese Journal of Acoustics* **15**, 314–318. Power flow transmission influenced by vibration source impedance in a compound system.
38. Y. P. XIONG and K. J. SONG 1996 *Chinese Journal of Mechanical Engineering* **9**, 13–20. Optimum control of vibration and structure-borne noise for machinery on flexible foundation.
39. Y. P. XIONG, J. T. XING and W. G. PRICE 1999 *Proceedings of the Asia-Pacific Vibration Conference* '99, Volume 2, 1227–1232. An active control method using power flow for vehicle–bridge interaction systems.
40. Y. P. XIONG and X. P. WANG 1998 *Chinese Journal of Experimental Mechanics* **13**, 243–246. Experimental study on power flow in machine-foundation flexible isolation system.
41. F. WANG 1997 *Master Thesis, Shandong University of Technology*. Experimental investigation of power flow for floating raft isolation systems (in Chinese).